

# NMR of membrane proteins in solution

Lukas K. Tamm <sup>\*</sup>, Binyong Liang

*Department of Molecular Physiology & Biological Physics, University of Virginia Health System,  
1300 Jefferson Park Avenue, Charlottesville, VA 22908-0736, USA*

Received 18 April 2006  
Available online 18 July 2006

**Keywords:** Membrane protein; NMR; Structure; Dynamics; Function; TROSY; Residual dipolar coupling; Paramagnetic; Relaxation; Spin label; Glycophorin A; Diacylglycerol kinase; KcsA; OmpA; OmpX; PagP; Phospholamban; Mystic

## Contents

1. Introduction	201
2. Membrane protein expression	202
3. Sample preparation in detergent micelles	202
4. Triple-resonance methods for assignment and structure calculation	203
5. Methyl-protonation	204
6. Long-range distances by paramagnetic relaxation enhancement	205
7. Refinement with residual dipolar couplings	206
8. Dynamics	206
9. Interactions with detergent molecules	208
10. Conclusion and outlook	209
References	210

## 1. Introduction

Solution NMR has been established as a major method to determine structures of proteins and protein complexes that are readily soluble in aqueous solution [1]. In addition to the elucidation of their structures, NMR also offers unique opportunities to probe dynamical processes of such proteins and complexes. Membrane proteins, when embedded in lipid bilayers, are not amenable to solution NMR techniques because their rotations in these environments are slow and highly anisotropic, which leads to unfavorable relaxation and very wide to undetectable resonance lines. However, solid-state NMR has been successfully employed to obtain highly resolved spectra of membrane-bound peptides and proteins in lipid bilayers. Solid-state NMR technology continues to be developed for membrane protein samples at a rapid pace and

the structures of several small proteins in lipid bilayers have been obtained by these methods [2,3]. An alternative approach to solving structures and obtaining dynamical information on membrane proteins is to extract the proteins from their host membranes and disperse them in non-denaturing micelles, which tumble fast enough to give well-resolved resonance lines when using solution NMR methods. Since, membrane protein–detergent complexes are usually still large on the scale of protein structures that are routinely solved by NMR, the most advanced solution NMR techniques and spectrometers operating at high magnetic fields are typically employed to solve structures of these membrane proteins. These include the use of transverse relaxation-optimized spectroscopy (TROSY) [4], labeling the proteins with two or three low-abundant isotopes, and obtaining structural restraints in addition to those typically obtained from nuclear Overhauser effects (NOEs) and chemical shifts, such as restraints obtained from residual dipolar couplings (RDCs) and paramagnetic relaxation enhancements (PREs). Here, we review the current status of solution NMR of membrane proteins. The focus is on recent developments that have made it feasible for solution NMR to successfully study the structure, dynamics, and function of this

<sup>\*</sup> Corresponding author. Tel.: +1 434 982 3578; fax: +1 434 982 1616.  
E-mail address: lkt2e@virginia.edu (L.K. Tamm).

important and abundant class of proteins, which is still hugely underrepresented in structural databases and is still largely excluded from ongoing structural genomics efforts. We illustrate technological advances in solution NMR of membrane proteins with several examples of new insights on membrane protein structure and function that have emerged in recent years by applying solution NMR to these systems. As is typical for progress in virtually all areas of structural biology, and particularly for the structural biology of membrane proteins, success depends on both advances in sample preparation and advances in structural methods. Therefore, the first two sections of this review are devoted to issues of sample preparation and the following sections touch on several solution NMR methods that have been successfully applied to expand our current knowledge of the structure and function of membrane proteins.

## 2. Membrane protein expression

The expression of membrane proteins on scales required for structural studies continues to be challenging. While expression levels of less than 1 mg of the desired protein per litre of culture may be acceptable for crystallization trials, especially when cultures can be grown on a large scale, much higher expression levels are needed to make heteronuclear NMR experiments economically feasible. Such restrictions appear to currently limit the expression of membrane proteins for NMR to *E. coli* and cell-free expression systems. Obviously, homologous prokaryotic expression is most straight-forward [5–7] and, indeed, most known membrane protein structures are of prokaryotic origin. Despite these successes, heterologous expression of eukaryotic membrane proteins in *E. coli* has also been successful and optimized for several classes of membrane proteins, including G-protein coupled receptors [8,9]. In most cases, proteins were expressed with His-affinity tags for purification on metal chelate columns. Often, but especially for relatively small membrane proteins, an N-terminal fusion of a secreted protein such as maltose-binding protein with its own signal sequence boosts expression and facilitates the correct insertion and folding into the cell membrane. Purification of small membrane proteins is also aided by expressing them as fusion proteins with a larger globular protein. These fusion proteins can later be cleaved by engineering a protease cut site between the globular carrier protein and the membrane protein. Useful protocols for screening the expression of membrane proteins in *E. coli* and their solubilization have been published [10]. Fusions with the membrane-associating protein *Mistic* have been reported to boost the expression of several membrane proteins, including voltage-gated potassium channels, growth factor receptors, and G-protein coupled receptors [19]. *Mistic* probably enhances the expression and folding of passenger membrane proteins by its ability to directly insert into the lipid bilayer of the cell membrane and thereby bypass translocon-assisted membrane protein insertion, which may be a bottleneck when expressing membrane proteins in the absence of *Mistic*.

An interesting alternative approach for the high-level expression of membrane proteins and their efficient isotopic labeling is to use cell-free extracts for expression. The ‘S30’ extracts from *E. coli* contain the complete transcription/translation system, but are depleted of endogenous mRNA and supplemented with nucleotide triphosphates, amino acids, T7-RNA polymerase and an energy regenerating system containing phosphoenol pyruvate and pyruvate kinase. Several transporters of the inner membrane of *E. coli* have been successfully expressed at levels of 1–2.7 mg/ml using this system [11]. Adding *E. coli* lipids increases the expression level about threefold, lyso-lipids have only a marginal effect, and the addition of several common detergents to the cell-free mix decreases expression. Although most proteins are expressed into insoluble fractions (especially in the absence of *E. coli* lipids), some of these fractions can be recovered by solubilization and refolding in various detergents. Similar levels of expression have been obtained with three different G-protein coupled receptors using the *E. coli* S30 extract [12]. Although to our knowledge not yet successfully used for membrane proteins, eukaryotic (e.g. wheat germ) cell-free extracts may also hold much promise for the efficient production of membrane proteins in relatively small volumes. An obvious advantage of cell-free expression systems is the relative ease of uniform and specific amino acid labeling. However, a potential danger is that the expressed proteins may not be correctly folded and that refolding into their native structure may be difficult. Therefore, it is very important to test the functional activity of the membrane protein samples that are produced by this method.

Beta-barrel membrane proteins are conveniently over-expressed in *E. coli* by deletion of the signal sequence and the consequent formation of inclusion bodies [13]. The material from inclusion bodies is denatured in urea or guanidium chloride, purified in an unfolded form and subsequently refolded into detergent micelles or lipid bilayers [14]. Several outer membrane proteins of *E. coli* have been successfully refolded and shown to regain function by using these procedures.

## 3. Sample preparation in detergent micelles

Over-expressed membrane proteins are typically purified on affinity columns. Different strategies have been successful for different membrane proteins. His-tags and metal chelation columns have perhaps been used most frequently, but maltose binding protein and amylose resins or glutathione transferase and glutathione columns have also been successfully used. The fused soluble affinity proteins are cleaved from the membrane protein of interest with specific proteases, which affords another purification step by size exclusion or ion exchange chromatography to remove the affinity protein and protease from the membrane protein sample.

There has been much debate about which detergents are best to prepare membrane protein samples for NMR study. Although it appears that no unique answer to this question benefits all membrane proteins, some common trends have

emerged from work in several laboratories. Well-resolved spectra of membrane proteins and particularly single trans-membrane peptides have been recorded in many instances in sodium dodecyl sulfate (SDS). Even though one often observes the highest numbers of resonances with the narrowest line-widths in SDS, it is not always clear that this harsh and denaturing ionic detergent maintains the native fold of membrane proteins. In favorable cases, SDS may be an acceptable detergent to analyze the structure of a single membrane-spanning helix or a very sturdy multi-helix membrane-spanning protein, but in most cases SDS partially denatures helical bundle membrane proteins, including bacteriorhodopsin and rhodopsin [15]. Krueger-Koplin et al. [16] found that SDS induces more than the expected number of cross-peaks in HSQC spectra of several membrane proteins, indicating that SDS may induce conformational heterogeneity. However, SDS may be very useful as an intermediate detergent to back-exchange amide protons in highly deuterated membrane protein samples (see below). A strategy to partially unfold the protein in SDS for back-exchange has been essential for the assignment of diacylglycerol kinase (DAGK) in dodecylphosphocholine (DPC) [17].

DPC has been quite popular in solution NMR studies of membrane proteins for probably three main reasons. First, it forms micelles of approximately 70–80 monomers, which corresponds to a molecular mass of approximately 25–28 kDa. Even if the molecular mass of the protein of interest is added, the size of the resulting complex is in a range that is tractable by solution NMR methods. Second, the chemical structure of the DPC headgroup closely mimics that of the most abundant phospholipids in lipid bilayers, i.e. phosphatidylcholines. It is zwitterionic and therefore provides a relatively mild environment for the embedded membrane protein. Third, the 12-carbon acyl chain is almost long enough to cover the hydrophobic surface area of a membrane protein in a similar fashion as phospholipids would in a lipid bilayer. NMR spectra of excellent quality have been obtained for quite a few membrane proteins with this detergent (see below), but its success has not been universal. There are cases of membrane proteins that are not stable in DPC for as long as in other, in most cases negatively charged phospholipid-mimicking detergents.

Another good detergent for several membrane proteins appears to be lyso-phosphatidylglycerol with a palmitoyl (LPPG), myristoyl (LMPG), or an oleoyl (LOPG) side-chain [16]. This detergent shares a natural lipid headgroup and a long hydrophobic chain with DPC. Lyso-PGs may be better than DPC in some cases because their negatively charged headgroups may keep highly concentrated micelle solutions that are often needed for NMR better apart and thereby prevent unfavorable micelle collisions and detergent/protein exchange. When the same proteins are reconstituted in the analogous lyso-phosphatidylcholines (PCs) fewer HSQC cross-peaks are observed and the samples are less stable in the long-term. It appears that for several proteins lyso-PCs offer no advantages over DPC [16]. However, LMPC may still be a good alternative to DPC for proteins that do not require a negatively

charged lipid to support activity or improve their long-term stability.

Dihexanoyl-phosphatidylcholine (DHPC) is a short-chain phospholipid with detergent properties. It has been successfully used in solution NMR studies of only a few membrane proteins, most notably OmpX. Although it has two acyl chains and is the most lipid-like, some membrane proteins do not keep well in this environment. We suspect that DHPC with its short chains is quite rapidly exchanging between individual micelles, which may not be a good property if the membrane protein of interest has some tendency to oligomerize or aggregate. The longer-chain phospholipids diC<sub>7</sub>PC and the even longer chain, but negatively charged diC<sub>8</sub>PG may still be good detergents that have not yet been explored for high-resolution work. Beyond these chain-length limits, these lipids first form larger aggregates and then bilayers and thus are unsuitable for solution NMR methods [18].

*N*-octyl- $\beta$ -D-glucopyranoside ( $\beta$ OG) and *n*-dodecyl- $\beta$ -D-maltoside (DDM) have also been successfully used in a few instances. Some, but by far not all membrane proteins behave well in these environments for NMR studies. Although these detergents do not mimic natural membrane components, they are very gentle and are proven excellent detergents in many purification protocols of membrane proteins. Despite these favorable properties, rapid exchange of monomers between micelles may become a problem at the high concentrations, elevated temperatures, and relatively long measuring times that are often needed in structural studies by NMR.

Lauryl dimethylamine oxide (LDAO) was used in the structure determination of *Mistic*. Of the commonly used detergents in membrane protein research, this detergent has one of the smallest headgroups with a quite polar N $\rightarrow$ O bond. Perhaps because of these attributes LDAO has been quite frequently used for the crystallization of membrane proteins. Although LDAO is a good detergent to get highly resolved NMR spectra of *Mistic* [19], it is apparently not a good detergent for NMR in the screens with three other membrane proteins performed by Krueger-Koplin et al. [16].

In conclusion, the experience with solution NMR studies of membrane proteins is still quite limited. Different micellar systems seem to work for different proteins and it is too early to make general recommendations with strong predictive power at this time.

#### 4. Triple-resonance methods for assignment and structure calculation

The usual triple-resonance methods may be applied to membrane proteins as commonly used to study soluble proteins. However, since most membrane protein-detergent complexes are quite large, TROSY versions of the HNCA, HN(CO)CA, HN(CA)CB, HNCO, HN(CA)CO, etc. experiments are used [20–23]. In all cases, where assignments of larger membrane proteins were complete or nearly complete, the spectra were recorded at a <sup>1</sup>H frequency of at least 700 MHz in order to achieve sufficient dispersion and resolution of the resonances. In addition, the <sup>13</sup>C nuclei

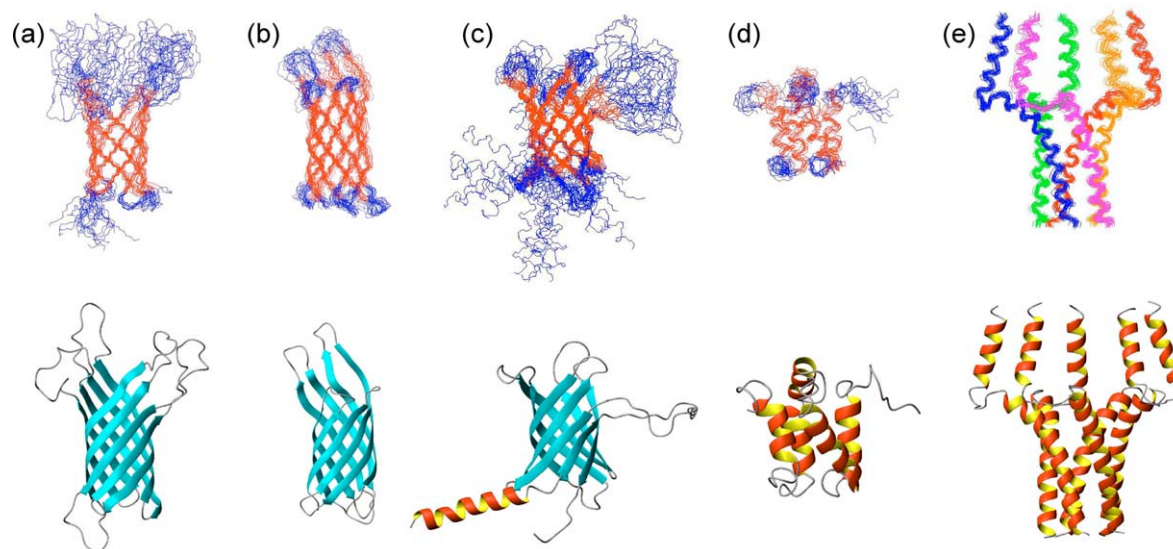


Fig. 1. NMR structures of five integral membrane proteins. (a) OmpA (PDB accession code 1G90 [25]), (b) OmpX (PDB accession code 1Q9F [32]), (c) PagP (PDB accession code 1MM4 [27]), (d) Mystic (PDB accession code 1YGM [19]), and (e) the phospholamban pentamer (PDB accession code 1ZLL [28]). Top row: ensemble structures. The well-defined secondary structures are colored red except for phospholamban where each subunit is labeled with a different color. Bottom row: ribbon representations of the closest-to-the-mean structures.

were deuterated by expression in D<sub>2</sub>O media supplemented with <sup>13</sup>C- and <sup>2</sup>H-labeled carbon sources, and only the amide protons were back-exchanged at moderately basic pH. Perdeuteration decreases dipolar interactions during transverse <sup>13</sup>C relaxation and thereby greatly improves the sensitivity and resolution of NMR spectra of large complexes [24]. Using these methods, complete or nearly complete backbone assignments have been obtained for three  $\beta$ -barrel membrane proteins, i.e. outer membrane protein A (OmpA) [25], outer membrane protein X (OmpX) [26], and PhoPQ-activated gene product P (PagP) [27], and for four  $\alpha$ -helical bundle proteins, i.e. diacylglycerol kinase (DAGK) [17], Mystic [19], pentameric phospholamban (PLB) [28], and the KcsA potassium channel [29]. Sometimes back-exchange of the amide protons of extremely stable trans-membrane helices is difficult to achieve. In this case, the protein may be expressed in H<sub>2</sub>O, but still with triple-labeled nutrients, which results in a protein with deuterated side-chain <sup>13</sup>C, but partially protonated main-chain <sup>13</sup>C and fully protonated amide <sup>15</sup>N nuclei [29]. Since, the resonances of the non-deuterated residues are much broader, but arise from well-structured regions, assignments of these have not been obtained using the usual suite of triple-resonance experiments, but rather through sequential connectivities obtained from <sup>15</sup>N-separated NOESY experiments. An alternative to perdeuteration is to deuterate at 85%, which has been sufficient to completely assign PLB (52-residue monomer) and Mystic (110 residues) [19,28].

<sup>15</sup>N-separated NOESY experiments were also used to obtain NOEs for secondary structure determination, and for the case of  $\beta$ -barrel membrane proteins, calculations of the global fold. Initial structures were calculated based on NOE-derived distance restraints and chemical shift (TALOS [30])-derived dihedral angle restraints. Approximately, 0.8–1.3

backbone NOE restraints and 1.2–1.9 dihedral angle restraints were collected per structured residue for the three  $\beta$ -barrel proteins that have been solved to date. In the case of Mystic and the PLB pentamer, 5.2 and 3.7 NOE restraints per residue had been used in the structure calculations, respectively, but most of these restraints were short- or medium-range. Only nine intermonomer NOE distances were found in the PLB pentamer and 29 long-range NOEs were measured in Mystic. Therefore, other methods had to be used for these helical proteins to obtain high-quality tertiary and quaternary folds (see below). For the case of  $\beta$ -barrel proteins, it is possible to improve the quality of the initial structure calculations by introducing additional inter-strand hydrogen bond restraints between those residues where inter-strand NOEs are experimentally observed. This type of refinement has been added to the structure calculations of OmpA (68 hydrogen bonds), OmpX (34 hydrogen bonds), and PagP (74–77 hydrogen bonds). The structures of five membrane proteins that have been solved by solution NMR methods are presented in Fig. 1. Of these, the structures of OmpA (Fig. 1(a)) and PagP (Fig. 1(c)) have been obtained by first calculating the folds with NOE distance and torsion angle restraints only and then refining the structures with hydrogen bond restraints where indicated by experimental NOEs.

## 5. Methyl-protonation

The sparse proton density in perdeuterated amide NH back-exchanged proteins leads to relatively few long-range NOEs and, as a consequence, to relatively poorly defined structures. A powerful method to reintroduce protons in an otherwise perdeuterated sample is to biosynthetically incorporate protonated methyl groups of leucine, valine, and isoleucine ( $\delta$ 1) by growing samples in minimal media with selectively labeled

$\alpha$ -ketoisovalerate and  $\alpha$ -ketobutyrate [31]. This method was successfully employed with OmpX [32]. The assignments were obtained from 3D (H)C(CC)-TOCSY-(CO)-[ $^{15}\text{N}$ , $^1\text{H}$ ]-TROSY and 3D H(C)(CC)-TOCSY-(CO)-[ $^{15}\text{N}$ , $^1\text{H}$ ]-TROSY experiments [33]. The proton and carbon resonances of all 32 L,V,I( $\delta$ 1) methyl groups of OmpX could be assigned in this manner. A large number of additional (526 vs. 107) NOEs and corresponding distance restraints were derived from these data and used to calculate a dramatically improved structure of OmpX. The rmsd of the backbone of the ordered  $\beta$ -barrel improved from  $3.11 \pm 0.32$  to  $1.42 \pm 0.16$  Å when these additional methyl NOE-derived distance restraints were included and further to  $1.17 \pm 0.15$  Å when 34 hydrogen bond restraints were added to the structure calculation. This structure is presented in Fig. 1(b).

Oxenoid and Chou used a combination of C(CO)NH and HC(CO)NH experiments and a  $^1\text{H}$ - $^{13}\text{C}$  HSQC experiment of a 10%  $^{13}\text{C}$ -labeled sample to assign all 48 methyl groups of PLB [28]. This less selective labeling scheme also included methyls from alanine, methionine and threonine, in addition to those from isoleucine, leucine, and valine. A total of 193 intra-monomer (HN–HN, HN–methyl, and methyl–methyl) distance restraints could be obtained by this procedure. Nine NOE-derived inter-monomer distance restraints, which each included one of these methyls, were also critical to define helix–helix associations and thus the pentameric structure of PLB, which is shown in Fig. 1(e). Since, the structures of the monomers were extremely well defined by a large number internal distance restraints, the nine distance restraints between subunits were sufficient to calculate a high quality structure of the homo-pentamer.

## 6. Long-range distances by paramagnetic relaxation enhancement

An alternative method used to obtain more distance restraints in the absence of a sufficient number of long-range NOEs is to measure long-range distances of protons to spin-labels that are introduced into specific sites by site-directed mutagenesis and sulfhydro-specific labeling with compounds such as 1-oxy-2,2,5,5-tetramethyl- $\eta^3$ -pyrroline-3-methyl-methanethiosulfonate (MTSSL; for chemical structure, see Fig. 2(b)) [34–36]. The rate of transverse relaxation of a proton nuclear spin is dramatically enhanced if it interacts with a nearby spin of an unpaired electron, such as the one present on the oxygen atom of MTSSL. This paramagnetic relaxation enhancement depends on the inter-spin distance to the sixth power ( $R_2^{sp} \sim r^6$ ) according to the well-known Solomon–Bloembergen equation for transverse relaxation [37]. Model calculations and experimental tests for protein complexes with a rotational correlation time of about 20 ns and Larmor frequencies of 500–800 MHz indicate that the method has the highest accuracy for determining distances in the 15–25 Å range [38]. Although the molecular correlation time does enter the Solomon–Bloembergen equation, the obtained distances are not critically dependent on a precise knowledge of  $\tau_c$ . Errors in the estimates of  $\tau_c$  of up to 40% may be tolerated to still obtain distances within the experimental accuracy of the measured inter-spin distances of  $\pm 2$  Å. Alternative to determining paramagnetic relaxation enhancements (PREs) by measurement of transverse relaxation times  $T_2$  (or equivalently spectral linewidths or intensities), distances could also be obtained from measurements of the PRE of

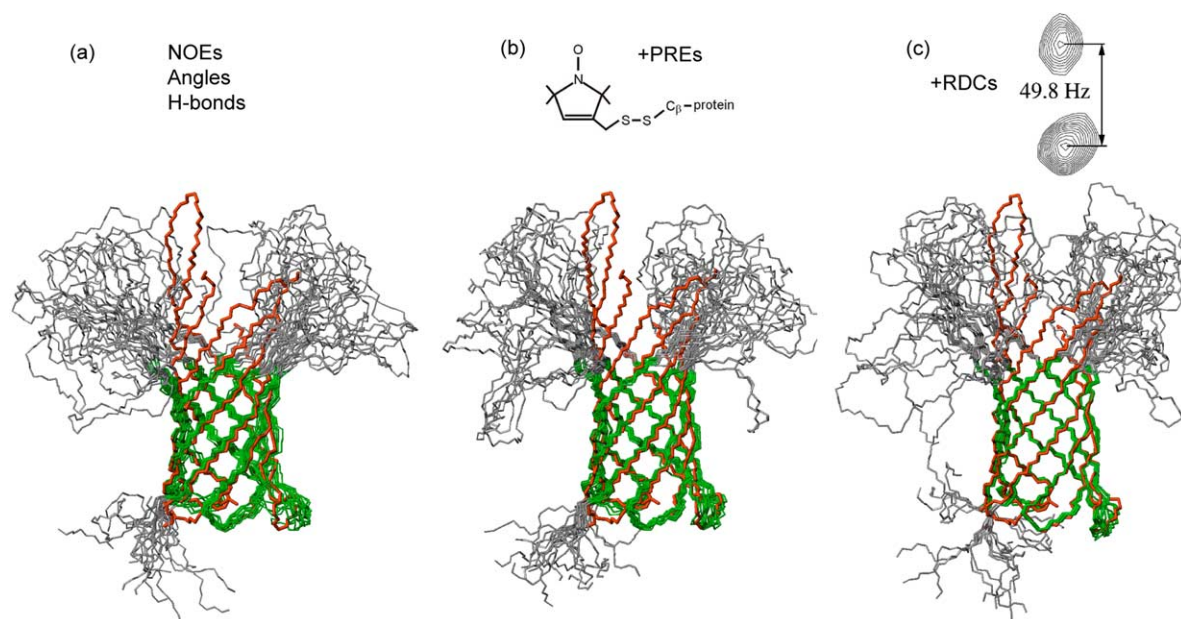


Fig. 2. Superposition of the ten lowest energy OmpA conformers calculated with (a) NOE, (b) NOE plus PRE, and (c) NOE plus RDC restraints, in addition to dihedral angle and H-bond restraints. Structured fragments used for the overlay are colored green. For comparison, the crystal structure (PDB accession code 1QJP [71]) is shown in red. The backbone rms deviations for the precision and accuracy of the green residues in the three ensembles are: (a)  $1.25 \pm 0.29$  and  $1.62 \pm 0.16$  Å, (b)  $0.85 \pm 0.17$  and  $1.09 \pm 0.12$  Å, and (c)  $0.62 \pm 0.16$  and  $1.11 \pm 0.06$  Å. Panels (a) and (b) reproduced with permission from Ref. [38]. The figure in panel (c) was recalculated using the data of Ref. [53], but employing the same criteria for structure calculation as those used to produce the structures shown in panels (a) and (b).

longitudinal relaxation times  $T_1$ . However, the values of  $T_1$  depend more critically on internal motions than the values of  $T_2$  and, therefore, such measurements are more critically dependent on local effective correlation times, which sometimes vary considerably in membrane proteins (see below).

An important factor for determining accurate distances by PREs is an accurate knowledge of the unperturbed, i.e. diamagnetic,  $T_2$  (or resonance linewidth or intensity) of each affected proton. A common method used to establish this reference value is to reduce the attached spin label by reducing agents such as ascorbate, sodium dithionite, or phenylhydrazine. However, we have found that it is difficult to completely reduce spin-labels that are attached to the membrane protein OmpA in several locations. A small fraction of the paramagnetic species persists even after extensive treatments with reducing agents, perhaps because the spin-labels are partially protected by detergent molecules of the surrounding micelle. This problem can be resolved by making two parallel samples, one labeled with the paramagnetic compound MTSSL and the other with the diamagnetic almost isosteric analog dMTSSL, in which the oxygen atom of MTSSL is replaced by an acetyl group. This approach was taken with the transmembrane domain of OmpA, which has no natural cysteines in its sequence. Eleven residues in different portions of the protein (hydrophilic, hydrophobic, interface) were individually changed to cysteines and labeled in parallel with MTSSL and dMTSSL. Ratios of the peak intensities and measurements of the linewidths of the resonances of the diamagnetically labeled samples gave values of  $R_2^D$ , from which 320 PRE distances could be obtained. Adding these 320 distance restraints to the calculations significantly increased the accuracy and precision of the structure of OmpA (Fig. 2(b)) [38]. It is even possible to obtain a reasonably well folded structure of OmpA with the PRE (and torsion angle) restraints only, i.e. in the absence of any NOE or hydrogen bond restraints [38].

Measurements of PREs obtained with MTSSL incorporated into five different sites were also used, and in fact needed, to determine the three-dimensional fold of the protein *Mistic* (Fig. 1(d)) [19]. In that work, the PRE data were not converted into actual distances, but the measured effects of the spin labels on the different protons were qualitatively classified and a total of 197 upper (at 19, 15, and 11 Å) and 290 lower (at 12, 16, and 20 Å) limit distance restraints were assigned. According to our experience with OmpA, the limits of 11 and 12 Å may be too tightly constrained and may have resulted in a more compactly folded protein than the actual shape that *Mistic* might adopt when bound to LDAO micelles. The hydrophilic surface and the relatively short helices of this purported membrane protein have perplexed many in the field.

## 7. Refinement with residual dipolar couplings

Measurements of residual dipolar couplings (RDCs) and their incorporation into structure calculations have been proven to dramatically enhance the accuracy and precision of the solution structures of a large number of soluble proteins [39–42] and a few small membrane proteins [43]. To measure

RDCs, the proteins need to be weakly aligned in an anisotropic solvent. Several methods are known to weakly align soluble proteins. They include lipid bicelles [44], filamentous phage [45], and compressed or stretched polyacrylamide gels [46–48]. Lipid bicelles that are commonly used for aligning soluble proteins are not appropriate for membrane proteins because they partition into these relatively large structures with a complete loss of all high resolution advantages to solve their structures. Opella's group has successfully measured RDCs of two single membrane-spanning helix proteins [49,50] and a membrane protein with two transmembrane helices [51] in compressed polyacrylamide gels. Bushweller and Cierpicki have developed a series of positively and negatively charged polyacrylamide-based copolymer gels that are suitable for the weak alignment of larger membrane proteins [52]. A good compromise between sufficient alignment and minimal signal broadening has been achieved in gels with 3–4% copolymer concentrations. Two of these gels, the 50% positively charged copolymer gel 50+M and the 50% negatively charged copolymer gel 50–S, which produce two distinctly different alignments of the protein/detergent complex, have been used recently to significantly improve the structure of OmpA in DPC micelles [53]. IPAP-HSQC and TROSY-based HNCQ-type experiments were used to measure  $^1D_{\text{HN}}$ ,  $^1D_{\text{C}'\text{C}\alpha}$ , and  $^1D_{\text{NC}'}$  couplings. Slightly more than 70 RDCs of each type and in each of the two aligning media amounting to a total of 434 RDCs were determined for residues located in the well-structured barrel and periplasmic turn regions of OmpA. Fitting of these RDCs to the high-resolution crystal structure of OmpA yielded good agreements with  $Q$ -factors of 27.2 and 26.1% for the 50+M and 50–S gels, respectively. Adding the 434 RDCs to the structure calculations improved the precision of the backbone structure of the structured fragment to a backbone rmsd of  $0.62 \pm 0.16$  Å and its accuracy to a backbone rmsd of  $1.11 \pm 0.06$  Å (Fig. 2(c)). A better definition of the periplasmic turns, where NOEs and dihedral angle restraints are sparser than in the barrel region is particularly evident in this refined structure [53].

A total of 115 RDC restraints have also been included in the calculation of the monomer of the highly defined subunit structure of PLB that is shown in Fig. 1(e) [28]. The backbone rmsd in this case was 0.61 Å. The RDC data consisted of 43  $^1D_{\text{HN}}$ , 31  $^1D_{\text{C}'\text{C}\alpha}$ , and 41  $^1D_{\text{NC}'}$  couplings that were measured by HNCQ-type experiments in a stretched 4% uncharged polyacrylamide gel.

## 8. Dynamics

NMR offers unique advantages for studying dynamical processes of macromolecules on many different time scales. Since, the function of biological macromolecules is often closely related to dynamical processes of individual or groups of residues, studies of the dynamics of these systems by NMR potentially can reveal much detail about their function. This general statement applies to membrane proteins just as well as to any other biological system. As structural biology of membrane proteins lags far behind similar efforts on

soluble proteins, detailed dynamical studies of membrane proteins that attempt to explain their functions are only at their very earliest stages. Although the dynamical properties of peptides that are bound to detergent micelles have been studied by NMR for quite some time, we focus here on dynamical studies of larger membrane proteins.

The three original descriptions of the structures of the three  $\beta$ -barrel membrane proteins OmpA, PagP, and OmpX all noted that the residues forming the extracellular loops of these proteins are much more disordered and much more dynamical than the residues forming the membrane-embedded  $\beta$ -barrel portions [25,27,32]. Some of the tight periplasmic turns are well ordered, but others are more dynamical. In OmpA, for example, turn 1 is more dynamical than turns 2 and 3 (see Fig. 2 in Ref. [54]). These and similar observations in the other two  $\beta$ -barrel proteins have been made by measuring heteronuclear  $\{^1\text{H}\}$ - $^{15}\text{N}$  NOEs and, in some cases,  $^{15}\text{N}$   $T_1$  and  $T_2$  relaxation times. Interestingly, recent measurements of RDCs of OmpA reveal that turn 1 and turn 3, but not turn 2 are conformationally heterogeneous as they can adopt two distinct conformations [53]. In the case of OmpX, the heteronuclear  $\{^1\text{H}\}$ - $^{15}\text{N}$  NOE measurements have been supplemented with measurements of the kinetics of amide hydrogen exchange [32]. Even though these two measurements probe the dynamics on very different time scales (picoseconds to nanoseconds vs. minutes), the overlapping maps show that the flexible loops move freely on the picoseconds to nanoseconds timescale, whereas the barrel is very stable over minutes and perhaps on even longer timescales.

The enzyme PagP found in the outer membrane of Gram-negative bacteria catalyzes the transfer of a palmitate chain from a phospholipid to the lipid A moiety of lipopolysaccharides. Crystallographic evidence shows that a single molecule of LDAO detergent is buried in the core of the barrel, perhaps indicating that it takes the place of the palmitate substrate. Since, the detergents that have been used to determine the structure of PagP by solution NMR ( $\beta\text{OG}$  and  $\text{DPC}$ ) are small enough to also fit into this cavity, it is likely that they are present in that location. This observation prompted Kay and collaborators to solve the structure of PagP in the presence of a detergent, CYFOS-7, that owing to its bulky cyclohexane ring does not fit into the cavity of PagP. They made the interesting observation that the protein existed in two slowly exchanging conformations under these conditions [55]. When the temperature of this sample was lowered to 25 °C, two sets of correlation peaks were found in the  $^1\text{H}$ - $^{15}\text{N}$  TROSY HSQC spectrum. The group managed the highly challenging task of almost completely assigning the residues of both conformations, T and R, even though T was present in the sample at only about 300  $\mu\text{M}$ ; the spectra are very crowded, and the resonances of the 50 kDa complex become quite broad at this temperature. The chemical shift and thus conformational differences between the T (tense, low temperature) and R (relaxed, high temperature) states are most significant in the extracellular loop between strands A and B, a bulge in strand A, and the portion of strand H that hydrogen-bonds to the bulge in strand A. This suggests that the bulge region may be the region that opens and

closes to let substrates in and out of the barrel and that this region and the adjacent loop may also participate in the catalytic action of this lipid-converting enzyme. The rates of conversion between T and R were measured at 25 °C via  $\text{N}_{\text{zz}}$  exchange spectroscopy [56]. At 45 °C, where only one set of  $^1\text{H}$ - $^{15}\text{N}$  correlations was observed, exchange rates were obtained via  $^{15}\text{N}$ -CPMG relaxation dispersion experiments [57,58]. Equilibrium constants describing the exchange equilibrium were obtained directly from the intensities of the  $^1\text{H}$ - $^{15}\text{N}$  correlation peaks at four more temperatures. The temperature dependence of the equilibrium constant describing the T  $\rightarrow$  R transition was thus determined by an enthalpy change of +10.7 kcal/mol and an entropy change of +37.5 cal/mol K. Enthalpy dominates the T state at low temperature ( $\sim 66\%$  populated at 15 °C) and entropy dominates the R state at high temperature ( $\sim 90\%$  populated at 45 °C). The  $k_{\text{TR}}$  interconversion rate for several residues is 5–7  $\text{s}^{-1}$  at 25 °C and  $\sim 300 \text{s}^{-1}$  at 45 °C. The reverse rates  $k_{\text{RT}}$  are  $\sim 3 \text{s}^{-1}$  and  $\sim 33 \text{s}^{-1}$  at 25 and 45 °C, respectively [55]. This example nicely illustrates the power of NMR to contribute to a deeper understanding of the function of membrane-bound enzymes.

Although OmpA is thought to have primarily a structural function, it has also been shown to form an ion channel in vitro and to affect the growth behavior of bacteria under stress situations in a manner that is consistent with OmpA forming a pore in vivo. The opening of the pore requires an opening of a channel-blocking salt-bridge formed by Arg 138-Glu 52 across the center of the barrel of OmpA. The dynamics of the transmembrane domain of OmpA have been investigated by NMR [59] (Blad, Abildgard, Arora, and Tamm, unpublished work). In these works,  $^{15}\text{N}$   $T_1$ ,  $^{15}\text{N}$   $T_2$ , and  $\{^1\text{H}\}$ - $^{15}\text{N}$  heteronuclear NOEs were measured each at three magnetic field strengths (500, 600, and 750 MHz proton frequency) and globally fitted to extract picoseconds and nanoseconds motions using the model-free approach [60,61] extended to anisotropically tumbling objects [62]. Two important results emerged from this work. First, the anisotropy of the rotational diffusion tensor of OmpA in DPC is inconsistent with the most likely physical shape of the protein/detergent micelle complex. Given the structure of OmpA and experiments discussed below, the lipids are expected to form a torus around the hydrophobic barrel surface. The axial ratio of the barrel axis relative to a perpendicular axis in this complex should not be significantly different from unity. However, the relaxation data indicate that OmpA rotates about 1.5 times faster about its long axis than about perpendicular axes. This has been interpreted in terms of a model in which OmpA rotates almost freely within the micelle along its barrel axis. The bound detergents appear not to contribute any significant drag to the axial rotation. Similar observations have been made with other smaller membrane proteins [16,63]. The second interesting result from the dynamics experiments on OmpA is that the long extended loop residues undergo fast fluctuating motions on the picoseconds time scale as well as collective motions on the nanoseconds time scale, whereas only fast picoseconds motions are observed for the residues that constitute the well-structured barrel. When the data were also analyzed for

possible contributions of conformational exchange,  $R_{ex}$ , to the transverse relaxation rate, several residues in the  $\beta$ -barrel were found to undergo conformational exchange on the microseconds to milliseconds timescale. A preview of this is shown in Fig. 2 of Ref. [59]. Most interestingly, the gate residue Arg 138 is one of those residues and Met 53, which is the next neighbor to gate residue Glu 52, is another residue that undergoes conformational exchange on the microseconds to milliseconds time scale, suggesting a mechanism of how this gate may open. When completed, this work could provide another nice example of how dynamical experiments by NMR can help explain the function of membrane proteins.

$^{15}\text{N}$   $T_1$  and  $T_2$  relaxation times have also been measured to establish that the PLB pentamer forms a stable structure and does not undergo significant chemical exchange by association and dissociation [28]. The authors show that the  $R_1R_2$  product is below a limiting value ( $<20 \text{ s}^{-2}$  at 600 MHz) throughout the structure, which is an approximate indicator of the absence of chemical or conformational exchange [64]. They also demonstrate that the  $R_2/R_1$  ratio is smaller in the N-terminal cytoplasmic than in the C-terminal transmembrane helices, indicating that the cytoplasmic helices are mobile relative to the transmembrane helices [65].

## 9. Interactions with detergent molecules

NMR is also an excellent method for studying the interaction of lipids and detergents with membrane proteins and thus mapping the regions of mutual contact. The literature contains a large body of studies, in which interactions between small membrane protein fragments and peptides and their micellar environment have been investigated by NMR, but these will not be reviewed here. We rather focus on interactions of larger protein/micelle systems. Wüthrich and collaborators have examined lipid–protein interactions in the OmpX/DHPC system in quite some detail [66,67]. In a first approach, intermolecular NOEs between the amide protons or the methyl protons of a selectively Leu, Val, and Ile methyl-protonated sample and various methyl and methylene resonances of DHPC were measured [66]. These measurements were performed with three-dimensional  $^{15}\text{N}$ -resolved [ $^1\text{H}$ – $^1\text{H}$ ] NOESY experiments to detect amide proton–lipid interactions and with 3D  $^{13}\text{C}$ -resolved [ $^1\text{H}$ – $^1\text{H}$ ] NOESY experiments (both at 800 MHz) to detect methyl proton–lipid interactions. Since, DHPC has short six-carbon acyl chains, the resonances of almost all methylene protons could be resolved. The resonances of the methyl protons at the ends of the apolar lipid tails and those of the polar choline headgroup are also well-resolved as expected. The choline methyls resonate at 3.16 ppm, the methylenes of carbons-2, -3, -4, and -5 at 2.21, 1.50, 1.22, and 1.22 ppm, respectively, whereas the terminal chain methyls of carbon-6 have a chemical shift of 0.78 ppm. NOE cross-peaks between amide protons and protons of the hydrophobic lipid side-chains cover the entire hydrophobic surface of OmpX and are restricted to that area. Therefore, these cross-peaks are good indicators for mapping interfaces of protein–lipid contact. Strong cross-peaks between lipid and protein methyl groups

were also observed in many locations throughout the hydrophobic surface of OmpX. Interestingly, some protein methyl groups that are located in a water-exposed loop have visible, albeit very weak cross-peaks to terminal lipid methyl groups, indicating that these lipids may on occasion also visit the hydrophilic parts of the protein. This suggests that the DHPC micelle, although predominantly forming a cylindrical shell around the hydrophobic portion of OmpX, exhibits a rather dynamic nature. NOE cross-peaks between methyl protons of the lipid choline headgroup and the protein are restricted to only a few sites near the hydrophobic–hydrophilic interface of the protein surface. These sites include a negatively charged glutamate and a couple of interfacial tryptophan residues. The lipid choline group is presumably attracted to negatively charged residues and to aromatic side-chains, which are well known to favorably partition into the interfacial regions of lipid bilayers [68]. The apolar and polar lipid–protein interactions together define the hydrophobic width of OmpX to be 28 Å, which is very similar to the hydrophobic width of the outer membrane of *E. coli* [69,70]. Since, the hydrophobic width of a bilayer of DHPC would be only about 16 Å, it was concluded that the lipid does not form a bilayer structure, but rather a torus-like monolayer around the hydrophobic surface area of the protein.

In a second approach, the same group used paramagnetic reagents of different lipid solubilities to map solvent (water and lipid) accessibilities of the protein surface [67]. Titrating the water-soluble  $\text{Gd}^{3+}$  complex Gd(DOTA) to the OmpX/DHPC complex enhances the transverse relaxation of amide protons that are exposed to the aqueous phase. The paramagnetic relaxation enhancements were measured with a 2D  $^{15}\text{N}$ ,  $^1\text{H}$ -TROSY experiment of a [ $^2\text{H}$ ,  $^{15}\text{N}$ ]-labeled sample and an analysis of the exponential decays of the cross-peak volumes as the concentration of the relaxation agent was increased. Essentially no lipid-covered residues, not even those covered predominantly by the polar headgroups, are affected by Gd(DOTA). This compound therefore maps the highly water-accessible extracellular loops and just a few periplasmic turn residues. Similar experiments were also carried out with two spin-labeled 18-carbon fatty acids, i.e. 5-doxyl stearic acid (5-DSA) and 16-doxyl stearic acid (16-DSA). The spin-labeled 5-DSA maps the entire hydrophobic surface of OmpX, i.e. almost exactly the same residues that are mapped by the amide proton–methyl/methylene proton NOEs described above. By contrast, the 16-DSA probe maps a narrower central apolar band around the perimeter of OmpX. This could be due to either the deeper hydrophobic location of this probe or the hydrophobic mismatch of the probe with the host lipid. Even if the direct measurements of NOEs perhaps give a more detailed picture of the lipid interactions in this complex, the paramagnetic method is very useful because it can be carried out with a double-labeled sample in a 2D experiment.

Chill et al. [29] measured the attenuation of the amide proton resonances of the KcsA channel as a result of the selective inversion of several proton resonances of the surrounding SDS micelles in a TROSY-based HNCOC experiment. Amide proton attenuations arising from NOEs from three

different selectively inverted spectral regions of the SDS  $^1\text{H}$  spectrum were obtained, namely those from the C2 methylene protons (1.5 ppm), the group of C3-11 protons (1.25 ppm), and the terminal methyl protons (0.85 ppm). Even with a mixing time of 250 ms, only moderate attenuations (up to 15% for C2 and C12 protons, up to 30% for C3-11 protons) were obtained. The attenuation by NOEs from the C3-11 protons cover the entire hydrophobic surface area of the protein. The attenuations from the C2 and C12 protons are smaller, but their more specific assignments provide valuable insight into the orientation of the detergents on the protein surface. The C2 protons of SDS attenuate two bands of amide protons in the region of the protein where the polar headgroups of the detergent are likely to make contact. Therefore, the C2 protons are good probes to map the polar/hydrophobic interface of the membrane protein. By contrast, the C12 protons of SDS attenuate amide protons in a central band of the protein that likely marks the region of the protein that makes contact with mid-plane of the membrane. An interesting effect is that protons at both, the outer N-terminal and the inner C-terminal helices of KcsA are attenuated by protons at the appropriate depth, even though the inner helix is supposed to be sheltered from contact with lipids according to the crystal structure. This was explained by a sporadic contact of a few inner helix residues with detergent protons and spin diffusion when NOEs were measured for a large complex with relatively long mixing times. Therefore, these methods likely map the exposure of protein segments rather than specific residues to the detergent micelle.

The contacts of the LDAO micelle with the surprisingly hydrophilic structure of Mistic were mapped by measuring detergent–protein NOEs and by using paramagnetic relaxation agents [19]. Although NOEs from the headgroup methyl protons of LDAO to the amide protons are preferentially located towards the two ends of the helical bundle, quite a few such NOEs are also found in the interior. Similarly, NOEs from the protons of the methyl groups at the hydrophobic tail end of LDAO are distributed along some of the helices. Paramagnetic relaxation enhancements by Gd(DOTA) are quite limited, and confined to the helical ends, whereas PREs by 16-DSA are spread throughout the molecule. Clearly, the separation of hydrophilic and hydrophobic domains of Mistic as assessed by these methods is not as clear-cut as in OmpX or KcsA.

## 10. Conclusion and outlook

It is clear that solution NMR of membrane proteins has a bright future. Significant progress has been made and several structures have been solved in recent years (Fig. 1) and more are on the horizon. In addition to structure determination, NMR also offers unique opportunities to sample dynamical properties of membrane proteins and thereby gain new insights into their functions. Lipid interactions can be studied by NMR in a perhaps more relevant environment than by crystallography because lipids (in micelles, bicelles, and membranes) provide a fluid rather than a solid solvent for this class of proteins. An

interesting prospect in this context is to supplement micelles or bicelles with a small ratio of long-chain to short-chain lipids with lipids of functional importance and study their interactions with membrane proteins. Finally, once solution NMR of membrane proteins becomes more routine, this method should add an extremely valuable tool to pharmaceutical efforts in drug discovery: more than half of all drugs currently on the market target membrane proteins and NMR already plays a major role in the development of drugs to soluble targets. Despite these exciting prospects, it is also clear that solution NMR of membrane proteins continues to be a challenging field and progress will come in measured steps. Challenges continue to exist in membrane protein expression and sample preparation as well as in NMR methodology. High-yield eukaryotic expression systems, in vivo or cell-free, that work well for membrane proteins would be particularly welcome. Expression in *Pichia pastoris* or wheat germ cell-free protein synthesis has been successfully employed to express soluble proteins for NMR and adaptation of these methods to membrane proteins is highly desirable. Expression in *E. coli* using Mistic fusions is also very promising because this method likely bypasses the bottleneck of the secretory machinery. There is continued need to improve membrane extraction and micellar sample preparation methods that are suitable for NMR. We suspect that expression into inclusion bodies and refolding of completely denatured membrane proteins from those will remain the exception rather than the rule to prepare properly refolded samples of functionally active membrane proteins for NMR. Sufficient consideration needs to be given to striking the best balance between protein conformational flexibility to allow back-exchange of the amide protons in highly deuterated membrane protein samples and the need to keep these samples in micelles that support their native structure. Different environments may need to be chosen for back-exchange and NMR measurements. An interesting possibility to overcome this problem in the future may be to go to completely carbon-based NMR techniques that are becoming increasingly popular with the new sensitivities that can be achieved with cryo-probes. The limited number of  $^1\text{H}$ – $^1\text{H}$  NOEs that are typically obtained using conventional techniques can be supplemented with long-range distance restraints from PREs of strategically placed spin-labels. Even a relatively poor initial structure obtained from a limited number of NOEs and/or PREs can be substantially refined using residual dipolar couplings. More progress also needs to be made with the assignments of side-chains and refinements of side-chain structure calculations. Novel computational and experimental methods are expected to improve this task. Finally, it is important to recognize that solution NMR structures in micelles are just that—NMR structures in micelles. Although it is likely that structures obtained by solution NMR in lipid micelles represent their structures in lipid bilayers quite well, especially when appropriate mild detergents are used, this needs to be verified. Solid-state NMR (and non-NMR) techniques can potentially provide this important link. It is therefore equally important to continue recent exciting developments in solid-state NMR of membrane

proteins, even if this was not the subject and emphasis of the current review.

## References

- [1] K. Wüthrich, *NMR of Proteins and Nucleic Acids*, Wiley, New York, 1986.
- [2] S.J. Opella, F.M. Marassi, *Chem. Rev.* 104 (2004) 3587.
- [3] O.C. Andronesi, S. Becker, K. Seidel, H. Heise, H.S. Young, M. Baldus, *J. Am. Chem. Soc.* 127 (2005) 12965.
- [4] K. Pervushin, R. Riek, G. Wider, K. Wüthrich, *Proc. Natl Acad. Sci. USA* 94 (1997) 12366.
- [5] M. Opekarova, W. Tanner, *Biochim. Biophys. Acta* 1610 (2003) 11.
- [6] D.N. Wang, M. Safferling, M.J. Lemieux, H. Griffith, Y. Chen, X.D. Li, *Biochim. Biophys. Acta* 1610 (2003) 23.
- [7] A. Korepanova, F.P. Gao, Y. Hua, H. Qin, R.K. Nakamoto, T.A. Cross, *Protein Sci.* 14 (2005) 148.
- [8] R. Grisshammer, J.F. White, L.B. Trinh, J. Shiloach, *J. Struct. Funct. Genomics* 6 (2005) 159.
- [9] A.A. Yeliseev, K.K. Wong, O. Soubias, K. Gawrisch, *Protein Sci.* 14 (2005) 2638.
- [10] C. Tian, M.D. Karra, C.D. Ellis, J. Jacob, K. Oxenoid, F. Sonnichsen, C.R. Sanders, *Methods Enzymol.* 394 (2005) 321.
- [11] C. Klammt, F. Lohr, B. Schafer, W. Haase, V. Dötsch, H. Rüterjans, C. Glaubitz, F. Bernhard, *Eur. J. Biochem.* 271 (2004) 568.
- [12] G. Ishihara, M. Goto, M. Saeki, K. Ito, T. Hori, T. Kigawa, M. Shirouzu, S. Yokoyama, *Protein Expr. Purif.* 41 (2005) 27.
- [13] M. Bannwarth, G.E. Schulz, *Biochim. Biophys. Acta* 1610 (2003) 37.
- [14] L.K. Tamm, H. Hong, B. Liang, *Biochim. Biophys. Acta* 1666 (2004) 250.
- [15] P.J. Booth, in: L.K. Tamm (Ed.) *Protein-Lipid Interactions: From Membrane Domains to Cellular Networks*. Wiley-VCH, Weinheim, Germany, 2005. p 57–80.
- [16] R.D. Krueger-Koplin, P.L. Sorgen, S.T. Krueger-Koplin, I.O. Rivera-Torres, S.M. Cahill, D.B. Hicks, L. Grinius, T.A. Krulwich, M.E. Girvin, *J. Biomol. NMR* 28 (2004) 43.
- [17] K. Oxenoid, H.J. Kim, J. Jacob, F.D. Sönnichsen, C.R. Sanders, *J. Am. Chem. Soc.* 126 (2004) 5048.
- [18] J.H. Kleinschmidt, L.K. Tamm, *Biophys. J.* 83 (2002) 994.
- [19] T.P. Roosild, J. Greenwald, M. Vega, S. Castronovo, R. Riek, S. Choe, *Science* 307 (2005) 1317.
- [20] M. Salzmann, K. Pervushin, G. Wider, H. Senn, K. Wüthrich, *Proc. Natl. Acad. Sci. USA* 95 (1998) 13585.
- [21] M. Salzmann, G. Wider, K. Pervushin, K. Wüthrich, *J. Biomol. NMR* 15 (1999) 181.
- [22] D. Yang, L.E. Kay, *J. Biomol. NMR* 13 (1999) 3.
- [23] D. Yang, L.E. Kay, *J. Am. Chem. Soc.* 121 (1999) 2571.
- [24] V. Tugarinov, P.M. Hwang, L.E. Kay, *Annu. Rev. Biochem.* 73 (2004) 107.
- [25] A. Arora, F. Abildgaard, J.H. Bushweller, L.K. Tamm, *Nat. Struct. Biol.* 8 (2001) 334.
- [26] C. Fernández, K. Adeishvili, K. Wüthrich, *Proc. Natl Acad. Sci. USA* 98 (2001) 2358.
- [27] P.M. Hwang, W.Y. Choy, E.I. Lo, L. Chen, J.D. Forman-Kay, C.R. Raetz, G.G. Privé, R.E. Bishop, L.E. Kay, *Proc. Natl Acad. Sci. USA* 99 (2002) 13560.
- [28] K. Oxenoid, J.J. Chou, *Proc. Natl Acad. Sci. USA* 102 (2005) 10870.
- [29] J.H. Chill, J.M. Louis, C. Miller, A. Bax, *Protein Sci.* (2006).
- [30] G. Cornilescu, F. Delaglio, A. Bax, *J. Biomol. NMR* 13 (1999) 289.
- [31] N.K. Goto, K.H. Gardner, G.A. Mueller, R.C. Willis, L.E. Kay, *J. Biomol. NMR* 13 (1999) 369.
- [32] C. Fernández, C. Hilty, G. Wider, P. Güntert, K. Wüthrich, *J. Mol. Biol.* 336 (2004) 1211.
- [33] C. Hilty, C. Fernández, G. Wider, K. Wüthrich, *J. Biomol. NMR* 23 (2002) 289.
- [34] J.R. Gillespie, D. Shortle, *J. Mol. Biol.* 268 (1997) 170.
- [35] V. Gaponenko, J.W. Howarth, L. Columbus, G. Gasmi-Seabrook, J. Yuan, W.L. Hubbell, P.R. Rosevear, *Protein Sci.* 9 (2000) 302.
- [36] J.L. Battiste, G. Wagner, *Biochemistry* 39 (2000) 5355.
- [37] I. Solomon, N. Bloembergen, *J. Chem. Phys.* 25 (1956) 261.
- [38] B. Liang, J.H. Bushweller, L.K. Tamm, *J. Am. Chem. Soc.* 128 (2006) 4389.
- [39] J.H. Prestegard, H.M. al-Hashimi, J.R. Tolman, *Q. Rev. Biophys.* 33 (2000) 371.
- [40] A. Bax, G. Kontaxis, N. Tjandra, *Methods Enzymol.* 339 (2001) 127.
- [41] A. Bax, *Protein Sci.* 12 (2003) 1.
- [42] E. de Alba, N. Tjandra, *Prog. Nucl. Magn. Reson. Spectrosc.* 40 (2002) 175.
- [43] D.H. Jones, S.J. Opella, *J. Magn. Reson.* 171 (2004) 258.
- [44] A. Bax, N. Tjandra, *J. Biomol. NMR* 10 (1997) 289.
- [45] G.M. Clore, M.R. Starich, A.M. Gronenborn, *J. Am. Chem. Soc.* 120 (1998) 10571.
- [46] H.J. Sass, G. Musco, S.J. Stahl, P.T. Wingfield, S. Grzesiek, *J. Biomol. NMR* 18 (2000) 303.
- [47] Y. Ishii, M.A. Markus, R. Tycko, *J. Biomol. NMR* 21 (2001) 141.
- [48] J.J. Chou, J.D. Kaufman, S.J. Stahl, P.T. Wingfield, A. Bax, *J. Am. Chem. Soc.* 124 (2002) 2450.
- [49] S.H. Park, A.A. Mrse, A.A. Nevzorov, M.F. Mesleh, M. Oblatt-Montal, M. Montal, S.J. Opella, *J. Mol. Biol.* 333 (2003) 409.
- [50] S. Lee, M.F. Mesleh, S.J. Opella, *J. Biomol. NMR* 26 (2003) 327.
- [51] S.C. Howell, M.F. Mesleh, S.J. Opella, *Biochemistry* 44 (2005) 5196.
- [52] T. Cierpicki, J.H. Bushweller, *J. Am. Chem. Soc.* 126 (2004) 16259.
- [53] T. Cierpicki, B. Liang, L.K. Tamm, J.H. Bushweller, *J. Am. Chem. Soc.*, in press. (*J.A.C.S. Vol.* 128 (2006), p.6947. DOI: 10.1021/ja0608343).
- [54] A. Arora, L.K. Tamm, *Curr. Opin. Struct. Biol.* 11 (2001) 540.
- [55] P.M. Hwang, R.E. Bishop, L.E. Kay, *Proc. Natl Acad. Sci. USA* 101 (2004) 9618.
- [56] N.A. Farrow, O. Zhang, J.D. Forman-Kay, L.E. Kay, *J. Biomol. NMR* 4 (1994) 727.
- [57] J.P. Loria, M. Rance, A.G. Palmer III, *J. Biomol. NMR* 15 (1999) 151.
- [58] F.A. Mulder, B. Hon, A. Mittermaier, F.W. Dahlquist, L.E. Kay, *J. Am. Chem. Soc.* 124 (2002) 1443.
- [59] L.K. Tamm, F. Abildgaard, A. Arora, H. Blad, J.H. Bushweller, *FEBS Lett.* 555 (2003) 139.
- [60] G. Lipari, A. Szabo, *J. Am. Chem. Soc.* 104 (1982) 4546.
- [61] G. Lipari, A. Szabo, *J. Am. Chem. Soc.* 104 (1982) 4559.
- [62] N. Tjandra, S.E. Feller, *J. Am. Chem. Soc.* 117 (1995) 12562.
- [63] J.J. Chou, J.L. Baber, A. Bax, *J. Biomol. NMR* 29 (2004) 299.
- [64] J.M. Kneller, M. Lu, C. Bracken, *J. Am. Chem. Soc.* 124 (2002) 1852.
- [65] L.E. Kay, D.A. Torchia, A. Bax, *Biochemistry* 28 (1989) 8972.
- [66] C. Fernández, C. Hilty, G. Wider, K. Wüthrich, *Proc. Natl. Acad. Sci. USA* 99 (2002) 13533.
- [67] C. Hilty, G. Wider, C. Fernández, K. Wüthrich, *ChemBiochem* 5 (2004) 467.
- [68] S.H. White, W.C. Wimley, *Annu. Rev. Biophys. Biomol. Struct.* 28 (1999) 319.
- [69] C.R. Raetz, C. Whitfield, *Annu. Rev. Biochem.* 71 (2002) 635.
- [70] S. Snyder, D. Kim, T.J. McIntosh, *Biochemistry* 38 (1999) 10758.
- [71] A. Pautsch, G.E. Schulz, *J. Mol. Biol.* 298 (2000) 273.